LANGMUIR

Article

pubs.acs.org/Langmuir

pH-Sensitive Poly(histidine methacrylamide)

Huifeng Wang,[†] Haiyan Wu,[†] Chen-Jung Lee,[†] Xia Lei,[†] Jiang Zhe,[‡] Fujian Xu,[§,∥] Fang Cheng,[⊥] and Gang Cheng*[,†]

[†]Department of Chemical and Biomolecular Engineering and [‡]Department of Mechanical Engineering, University of Akron, Akron, Ohio 44325, United States

[§]Key Laboratory of Carbon Fiber and Functional Polymers, Beijing University of Chemical Technology, Ministry of Education, Beijing 10029, China

[∥]Beijing Laboratory of Biomedical Materials, Beijing University of Chemical Technology, Beijing 100029, China

[⊥]School of Pharmaceutical Engineering, Dalian University of Technology, Dalian, Liaoning Province, 116024, China

ABSTRACT: This research reports a synthetic amino acid based zwitterionic poly(histidine methacrylamide) (PHisMA), which possesses switchability among zwitterionic, anionic, and cationic states, pH-dependent antifouling properties, and chelation capability to multivalent metal ions. The PHisMA polymer brush surface shows good antifouling properties to resist protein adsorption and bacterial attachment in its zwitterionic state at pH 5. This study also demonstrates that the solution acidity significantly affects the mechanical properties of PHisMA hydrogels. PHisMA hydrogels show higher viscoelastic properties and lower swelling ratios in the zwitterionic state at pH 4 and pH 5, compared to higher or lower pH conditions. It was discovered that PHisMA can chelate multivalent metal ions, such as Ca^{2+}, Mg^{2+}, Cu^{2+}, Ni^{2+} and Fe^{3+}. This study provides us a better understanding of structure−property relationships of switchable zwitterionic polymers. PHisMA can potentially be adapted for a broad range of applications including wound care, water treatment, bioseparation, coating, drug and gene delivery carriers, etc.

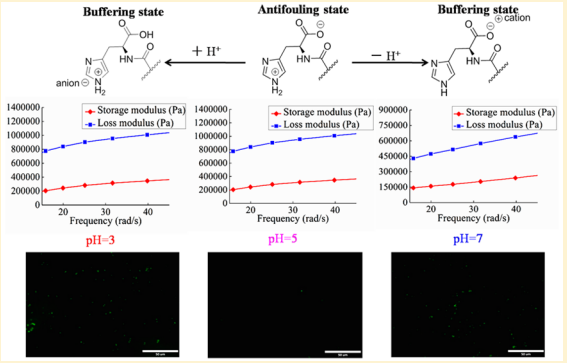

1. INTRODUCTION

Over the past 20 years, antifouling materials have attracted considerable attention from many applications, such as coating,[1] biomedical devices,[2−4] drug and gene delivery carriers,[5−9] membranes and protein purifications,[10−12] biosensors,[13−15] and wound dressings.[16] Antifouling materials, which can respond to environmental stimuli (such as pH, ionic strength, or temperature), have many advantages over sole-functional antifouling materials.[17−22] Among antifouling materials, poly(ethylene glycol) (PEG) and its derivatives are commonly used due to their steric exclusion effect and surface hydration to repel biomacromolecules.[18,23−28] However, PEG is susceptible to oxidation degradation and likely to lose its protein repulsive properties at high temperatures.[29,30] Due to their excellent antifouling properties, structure flexibility and tunable properties, zwitterionic polymers have emerged as a group of promising ultralow fouling materials.[18,29,31] Among zwitterionic materials, amino acid based polymeric materials have several advantages due to their unique structures containing pH sensitive anion (carboxylate) and cations (primary or secondary amines).[32] Moreover, amino acid side chains can improve the aqueous solubility of polymers and promote a higher order structure through intra- and interchain interaction via noncovalent forces such as hydrogen bonding, hydrophobic stacking and electrostatic interactions.[33−38] In existing amino acid based zwitterionic materials, primary/secondary amines respond to pH changes at basic conditions (pH 9−12). In many applications, such as wound healing, gene delivery and antimicrobial applications, materials that can respond to pH at neutral and slightly acidic conditions are needed. In our previous study, we developed two zwitterionic carboxybetaine polymers carrying tertiary amines as the cation,[39] which have buffering capacities at pH 7−9.

The object of this work is to develop a pH-responsive zwitterionic poly(histidine methacrylamide) (PHisMA) that can respond to pH at acidic (5−6) conditions and understand the structure−property relationships of PHisMA under different pH conditions. Due to the unique properties of imidazole group, PHisMA is expected to be sensitive to pH in a biologically relevant range compared to the other pH sensitive zwitterionic polymers. PHisMA polymer brushes were synthesized on the gold substrate by surface-initiated photoiniferter-mediated polymerization (SI-PIMP). The properties of PHisMA at different pHs to resist protein absorption and cell adhesion were studied. The viscoelastic properties and water uptake of PHisMA hydrogels are also investigated under

Received: April 15, 2016
Revised: May 31, 2016

DOI: 10.1021/acs.langmuir.6b01465
Langmuir XXXX, XXX, XXX−XXX

different pH conditions. Moreover, the chelating capability of PHisMA hydrogel to high-valent (+2 and +3) metal cations was determined.

2. EXPERIMENTAL SECTION

2.1. Chemicals. L-Histidine (≥99%), sodium sulfate (≥98%), acetone (≥99.5%), 2-propanol (≥99.5%), tetrahydrofuran (THF) (≥99%), 2-hydroxy-4′-(2-hydroxy-ethoxy)-2-methylpropiophenone (98%), *N*,*N*′-methylene-bis(acrylamide) (99%), phosphate buffered saline (PBS), nickel(II) sulfate hexahydrate (99%), dioxane (≥99.0%), and lysozyme (from chicken egg white, 53 000 units/mg) were purchased from Sigma-Aldrich (St. Louis, MO). Methacrylic anhydride (94%), copper(II) chloride dihydrate (98%), and iron(III) chloride anhydrous (98%) were purchased from Alfa-Aesar (Ward Hill, MA), and 2,2′-azobis[2-(2-imidazolin-2-yl)propane] dihydrochloride (VA-044) was purchased from Wako Chemicals USA (Richmond, VA). Hydrochloric acid (36.5−38%) and ethyl ether (99.0%) were purchased from EMD Chemicals (Darmstadt, Germany). Ethanol was purchased from Decon Laboratories, Inc. Pepsin (from porcine gastric mucosa, 10 635 units/mg) was purchased from Chem-Impex Int'l. Inc. (Wood Dale, IL).

2.2. Synthesis and Characterization of Histidine Methacrylamide and Poly(histidine methacrylamide). Histidine methacrylamide (HisMA) was synthesized based on the previously reported synthetic method.[40] L-Histidine (10 g, 64 mmol) was dissolved in 2 N NaOH (40 mL) aqueous solution and cooled in an ice bath. Methacrylic anhydride (30 mL, 195 mmol, 3 equiv) was dissolved in 80 mL of dioxane. The methacrylic anhydride solution was added to the aqueous solution of L-histidine dropwise in a 500 mL three-necked round-bottom flask under nitrogen protection. During the addition, the reaction mixture was kept in an ice bath. Then the mixture was reacted overnight at room temperature. After the reaction, dioxane was evaporated and hydrochloric acid was added until the solution reached pH 2. The residue chemicals and byproducts were removed by ether extraction three times. The pH value of the aqueous solution was adjusted to 5 using 2 N NaOH. The product was extracted with ethanol. By this process, L-histidine and NaCl were removed. The ethanol was evaporated and mixed with an excess of acetone. The product HisMA precipitated in acetone, and it was then vacuum-dried overnight. A 10.7 g sample of HisMA was obtained at a yield of 75%. ^{1}H NMR (300 MHz, D_2O) 1.83 (s, 3H, $CH_3C(=CH_2)H-$), 3.01−3.28 (m, 2H, $-CH_2$-imidazole), 4.47−4.51 (q, H, $-NHCH(COOH)-CH_2-$), 5.37−5.58 (m, 2H $-CH_2C(CH_3)-$), 7.17 (s, 1H imidazole, $-C=CHN=$), 8.48 (s, 1H imidazole, $-N=CHNH-$).

Poly(histidine methacrylamide) (PHisMA) was synthesized via the thermally initiated free radical polymerization method. The water-soluble thermal initiator VA-044 (2,2′-azobis[2-(2-imidazolin-2-yl)-propane] dihydrochloride) (0.03 g, 0.09 mmol) and HisMA monomer (2 g, 9 mmol) were dissolved in 20 mL of ultrapure water in a 100 mL round-bottom flask under nitrogen protection. The polymerization proceeded for 24 h at 50 °C. After 24 h, the solution was cooled to room temperature and then dialyzed in water with molecular weight cutoff of 10 kDa for 2 days. The product was then lyophilized for 2 days. Gel permeation chromatography (GPC) was carried out using an SEC gel column (Agilent Technologies, Santa Clara, CA) and an internal refractive index (RI) detector (Waters Corp., Milford, MA). For PHisMA, running buffer (containing 0.01 M NaH_2PO_4 and 0.3 M $NaNO_3$) was used as the eluent at a flow rate of 1 mL/min at 25 °C. The molecular weight (MW) was 10 986 g/mol.

2.3. Titration of HisMA and PHisMA. 5 mL of HisMA and PHisMA solutions at a concentration of 0.1 M were prepared in deionized water, and the solutions were adjusted to pH 1 using hydrochloric acid. Then the solutions were titrated against 0.25 N NaOH solution by adding 20 μL of NaOH solution each time until the pH reached 13. The change in pH was monitored by a pH meter.

2.4. Preparation of Photoiniferter-Coated Surface Plasmon Resonance (SPR) Chips. Before the formation of a self-assembled monolayer (SAM) of the photoiniferter 11-mercaptoundecane-1-[4-({[(diethylamino)-carbonothioyl]thioethyl}phenyl)carbamate] (DTCA) on the gold-coated SPR chips, the SPR chips were washed with acetone, isopropanol, and water, cleaned with a UV-ozone cleaner for 20 min, washed with water and ethanol, and then dried under a stream of filtered air. Subsequently, SPR chips were soaked in THF solution containing 0.1 mM photoiniferter at room temperature for 24 h. Prior to the polymerization, the SPR chips were rinsed with THF and then dried with a stream of filtered air.

2.5. Surface Initiated Photoiniferter-Mediated Polymerization (SI-PIMP). The monomer solution was first prepared by dissolving 0.5 g of HisMA in 10 mL of PBS at pH 8.5. The solution was deoxygenated by passing a continuous stream of nitrogen through the liquid for 20 min. The gold chip with photoiniferter SAM was placed into a quartz tube under nitrogen protection. After 20 min, the monomer solution was transferred to a quartz tube using a syringe and then a stream of nitrogen was purged into the reaction tube for another 5 min before being removed and covered with aluminum foil. Subsequently, the quartz tube containing the SPR chip and monomer solution was irradiated under 302 nm UV light (UVP, Model UVM-57). A 280 nm cutoff filter was put between the reaction tube and UV lamp to avoid the cleavage of the thiol−gold bond of the photoiniferter SAM.[41,42] After 2 h, the SPR chip was removed, washed with PBS, and put into PBS solution overnight before SPR study.

2.6. Measurements of Nonspecific Protein Absorption by SPR. All SPR experiments were performed at 25 °C using a four-channel SPR sensor (PLASMON-IV, Institute of Photonics and Electronics, Academy of Science, Czech Republic). The changes of resonance wavelength were measured by the SPR sensor at a fixed light incident angle. All buffers were freshly prepared, filtered using 0.2 μm syringe filters, and degassed. The PHisMA-coated SPR chip was attached to the base of the prism. The refractive index matching fluid (Cargille) was used as an optical contact between two surfaces. After first establishing a preabsorptive baseline using PBS at a flow rate of 50 μL/min under ambient temperature, the protein adsorption in the lysozyme solution (1 mg/mL) and pepsin solution (1 mg/mL) at different pHs (pH 3, pH 5 and pH 7) was studied. The amount of adsorbed proteins was calculated from the change in wavelength before and after protein injection. A 1 nm SPR wavelength shift is equivalent to 15 ng/cm^2 adsorbed protein.[20]

2.7. Bacteria Attachment. The method for evaluating the antibacterial efficiency of polymer surfaces was based on a previously reported method.[43,44] *E. coli* K 12 was first cultured in Luria−Bertani (LB) medium (20 g/L). The cultures were incubated at 37 °C with shaking at 200 rpm overnight to reach an optical density of 0.8 at 600 nm. Cell pellets were washed three times with sterile PBS (pH 7.4) and subsequently suspended in PBS to obtain a final concentration of 10^9 cells/mL. A 100 μL volume of *E. coli* suspension was dropped onto gold-coated glass slides with grafted polymer brushes, which were then covered with clean microscope slides. The polymer brush surfaces were preplaced into buffers with different pH values (pH 3, pH 5, and pH 7) to reach a stable charged state. The samples were stained with 100 μL of LIVE/DEAD BacLight Bacterial Viability assay (Thermal Scientific, Waltham, MA, USA) solution and then incubated at room temperature for 1 h. The cover slides were removed, and the samples were placed in Petri dishes containing 5 mL of buffers with different pH values at 37 °C with gentle shaking for 1 h in order to wash the detached bacteria. The amount of attached cells was determined using an Olympus IX81 fluorescence microscopy with 60× oil lens through FITC and Cys3 filters. Three samples were analyzed for each gold substrate separately.

2.8. Preparation of Hydrogels. Chemically cross-linked hydrogels were prepared via photoinitiated free radical polymerization in 1 mL of water at different pH values (pH 3, pH 4, pH 5 and pH 7). First, 6.68 mg of photoinitiator, 2-hydroxy-4′-(2-hydroxy-ethoxy)-2-methylpropiophenone, was dissolved in water by sonicating at 40 °C. Then 11.56 mg of cross-linker, *N*,*N*′-methylene-bis(acrylamide), was added into the initiator solution and sonicated in an ice bath to avoid gel formation between photoinitiator and cross-linker. After the solution became clear, 0.336 g of HisMA monomer was added to the solution. After the filtration by a 0.2 μm filter, the solution was added

DOI: 10.1021/acs.langmuir.6b01465
Langmuir XXXX, XXX, XXX−XXX

Scheme 1. Synthetic Route of HisMA

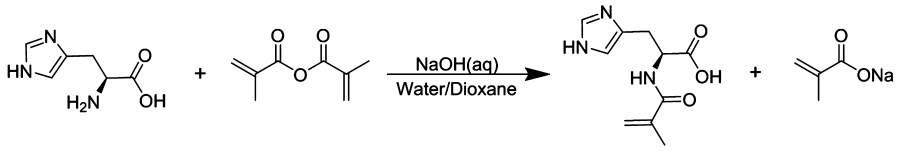

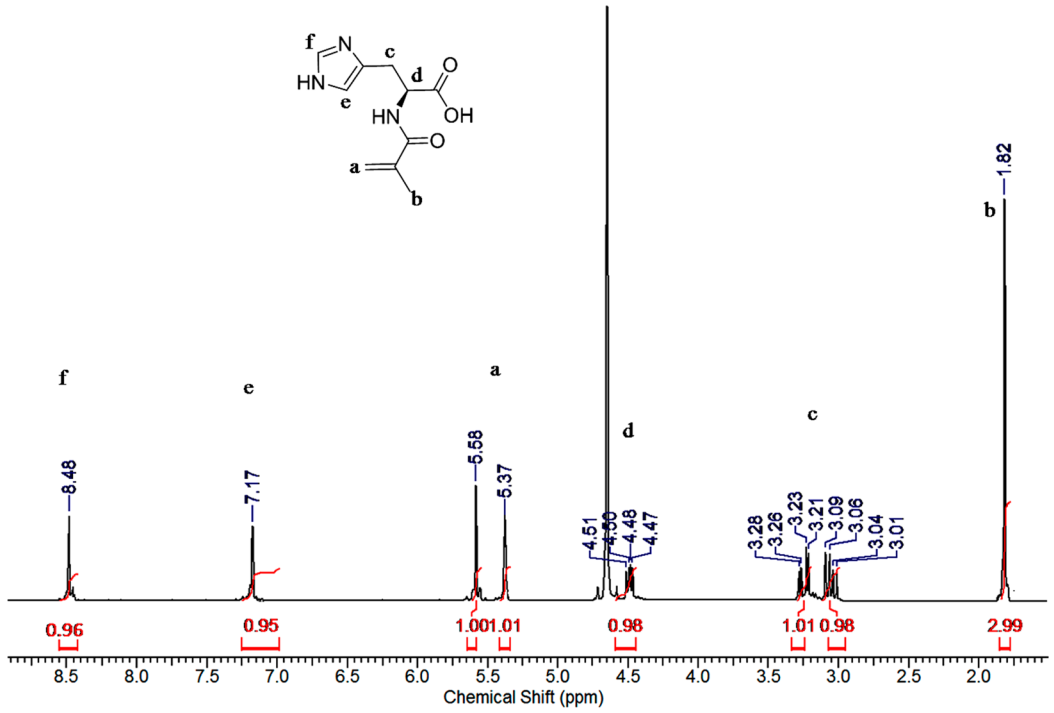

Figure 1. ^{1}H NMR spectrum for HisMA.

to the model with 25 mm diameter. The obtained hydrogels were 25 mm in diameter and 2 mm in height.

2.9. Rheological Studies. The in situ rheological studies were used to access the viscoelastic properties of PHisMA hydrogels. PHisMA hydrogels were equilibrated in the buffer at different pH values overnight. Measurements were performed at ambient temperature with a frequency of 1 rad/s and a strain of 10%. PHisMA hydrogels were loaded between 25 mm parallel plate geometry on a TA Instruments ARES-G2 rheometer. The frequency for different samples was based on the gel network structure. The storage modulus and loss modulus were monitored during the measurement process.

2.10. Swelling Ratio Measurement. For swelling ratio studies, PHisMA hydrogels were made 25 mm in diameter and 2 mm in height in buffers with different pH values via photopolymerization. After swelling equilibrium in ultrapure water overnight, the weight of PHisMA hydrogels was recorded and then the hydrogels were placed in a freeze-dryer and lyophilized prior to being weighed again. The swelling ratio, Q, was calculated using the following equation.

$$Q = W_S/W_D \times 100\%$$

where W_S is the weight after swelling and W_D is the weight after lyophilizing.

2.11. Metal Ion Chelation Studies. For chelation studies, PHisMA hydrogels were prepared 8 mm in diameter and 2 mm in height in ultrapure water. Then, PHisMA hydrogels were lyophilized and weighed. Subsequently, gels were immersed into ultrapure water to reach the swelling equilibrium and submerged into 1 M copper(II) chloride, nickel(II) sulfate, calcium chloride, magnesium sulfate, and ferric chloride solutions, respectively, to chelate metal ions. After 24 h, the equilibrated PHisMA hydrogels were placed into ultrapure water to release unbounded metal ions prior to being lyophilized and weighed again. The binding capacity of PHisMA hydrogel (D) to Cu^{2+}, Ni^{2+},Ca^{2+}, Mg^{2+}, or $Fe^{3+}$was calculated using the following equation.

$$D = ((W_C - W_D)/M_w)/W_D$$

where W_C is the dry weight of the hydrogel after chelating with Cu^{2+}, Ni^{2+}, Ca^{2+}, Mg^{2+}, and Fe^{3+}; W_D is the dry weight of PHisMA hydrogel before the chelation; and M_w is the molecular weight of the corresponding salt.

3. RESULTS AND DISCUSSION

As shown in Scheme 1, HisMA was synthesized via a one-step reaction. The chemical structure was characterized by ^{1}H NMR spectroscopy (Figure 1). Since the pK_a of acid/base groups in a zwitterion determines its charged state under different pH conditions, the pK_a values of the carboxylate and imidazole groups of HisMA were measured by titration. As shown in Figure 2, the monomer and polymer titration study revealed pK_a values of 1.82 and 6.12 for the carboxylate and imidazole groups, respectively, which are consistent with those in histidine.[45] At low pH conditions (pH <1.82), both carboxylate and imidazole groups are protonated, which leads to cationic HisMA and PHisMA. Between pH 1.82 and pH 6.12, both carboxylate and imidazole are partially charged. HisMA and PHisMA have balanced charges, and they have properties of zwitterionic molecules. At higher pH conditions (pH >6.12), most carboxylate and imidazole groups are deprotonated, and HisMA and PHisMA become anionic. In zwitterionic molecules, the acidity of carboxylate and the basicity of amine are affected by the distance between carboxylate and

DOI: 10.1021/acs.langmuir.6b01465
Langmuir XXXX, XXX, XXX−XXX

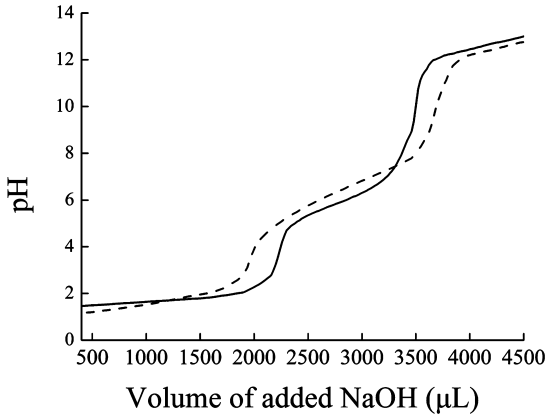

Figure 2. pH titrations of HisMA (solid line) and PHisMA (dashed line) from pH 1 to 13.

amine, the density of the charged groups and the substitution group of the amine.[39] It was found that the acidity of carboxylate increases with the decrease in the carbon spacer between amine and carboxylate. The charge state of the molecule significantly affects the interaction of molecules with solvent, salt, macromolecules, and itself, which subsequently will change the antifouling, mechanical, and other physical properties of the material.

In complex biological systems, the property of a material or device to resist the adsorption of biomacromolecules is critical for its interaction with cell, service life and performance. To evaluate antifouling properties under three charged states, PHisMA polymer brushes on gold substrate were prepared via surface-initiated photoiniferter-mediated polymerization. The pH-dependent single protein absorption on PHisMA surfaces was studied between pH 3 and pH 7 by a surface plasmon resonance (SPR) sensor. Lysozyme with an isoelectric point (p*I*) of 11.35 and pepsin with a p*I* of 2.2−3.0 were used as the model proteins. These proteins were chosen as their contrast charged states in the pH 3−7 range. Lysozyme was positively charged while pepsin formed the negatively charged counterpart over the entire pH range in our study. Table 1 shows that the adsorption of both proteins on PHisMA polymer brush surfaces at pH 3 and pH 7 were much higher compared to pH 5, which suggested PHisMA was under different charged states. At pH 3, the protonation of the imidazole group and partial protonation of carboxylate switch the polymer surface to be cationic and the negatively charged pepsin adsorbed more than that at pH 7, whereas the positively charged lysozyme adsorbed at pH 3 less than that at pH 7. At pH 7, the deprotonation of carboxylate and imidazole made the surface anionic and positively charged lysozyme adsorbed more compared to pH 3. PHisMA polymer brush surfaces showed better protein resistance at pH 5 with 0.5 ng/cm^2 lysozyme and less than 0.3 ng/cm^2 pepsin, suggesting a balanced charge state in this pH range. The results from pepsin and lysozyme absorption indicate that the PHisMA surface can switch among cationic, zwitterionic and anionic states by changing the pH of the solution.

Table 1. Pepsin and Lysozyme Absorption on PHisMA Surfaces under Different pH Conditions (pH 3, pH 5, and pH 7)

	pH 3	pH 5	pH 7
pepsin adsorption (ng/cm^2)	8.0	≪0.3[a]	0.5
lysozyme adsorption (ng/cm^2)	2.5	0.5	10.0

[a]Detecting limit.

Tunable antimicrobial and antifouling properties are very useful for medical device coatings and wound dressings. Due to the distinct surface charges under different pH conditions, PHisMA was expected to catch cells at low pH conditions and resist the attachment of cells at an intermediate pH range. Bacterial cell attachment onto PHisMA polymer brush surfaces was investigated using *E. coli* K12 as a model cell. *E. coli* K12 at the concentration of 10^9 cells/mL was incubated with PHisMA polymer brush surfaces in buffers at different pH values (pH 3, pH 5 and pH 7) as shown in Figure 3, a very small number of cells were observed on PHisMA surfaces in pH 5 buffer after culturing overnight. In contrast, more *E. coli* K12 cells attached on PHisMA surfaces in pH 3 and pH 7 buffers. The cell densities on the surface were $(46.24 \pm 2.43) \times 10^4$, $(0.76 \pm 0.47) \times 10^4$ and $(27.59 \pm 2.25) \times 10^4$ cells/cm^2, respectively, at pH 3, pH 5 and pH 7. PHisMA surface at pH 5 has the best antifouling property to resist bacterial attachment. PHisMA surface at pH 7 shows higher bacterial attachment, although both the surface and *E. coli* K12 are negatively charged under this condition. It should be noted that the adhesion/adsorption of cells/biomolecules to the surface is determined by all interactions including electrostatic, hydrogen bond and van der Waals interactions. A similar phenomenon was explained according to electrostatic interactions and between cells and surfaces, as described by DLVO theory.[46] Our study also demonstrates that zwitterionic surfaces are by far the most reliable antifouling surfaces under all tested conditions. The protein absorption and bacteria attachment results illustrate that the antifouling/fouling properties of PHisMA polymer brushes can be tuned over the pH range that is more relevant to biological conditions.

Hydrogels are widely used in many biomedical and biotech applications due to their high water content, tunable and

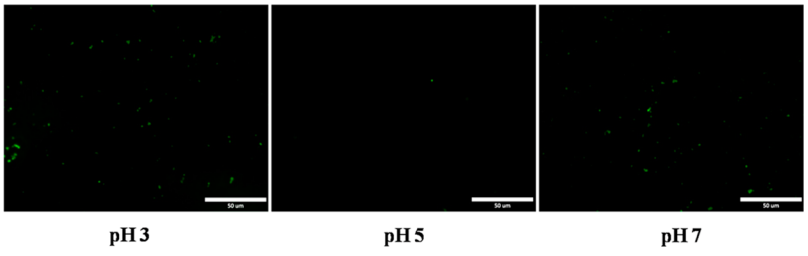

Figure 3. Bacterial attachment on PHisMA polymer brush surfaces under different pH environments. The scale bar is 50 μm. The cell densities on the surface were $(46.24 \pm 2.43) \times 10^4$, $(0.76 \pm 0.47) \times 10^4$, and $(27.59 \pm 2.25) \times 10^4$ cells/cm^2, respectively, at pH 3, pH 5 and pH 7.

DOI: 10.1021/acs.langmuir.6b01465
Langmuir XXXX, XXX, XXX−XXX

comparable mechanical properties to tissues, biocompatibility, etc. Many of these properties are determined by the interaction among polymer chains. Zwitterionic polymers typically show antielectrolyte properties. Electrolytes/salts screen the attractive interaction among cations and anions. At the presence of the electrolytes/salts, the zwitterionic polymer exists in a more stretched conformation. In contrast, the electrolytes/salts screen the repulsive interaction among the solely charged side chains in cationic or anionic polymers, so cationic and anionic polymers will switch from the stretched state to the random coils in the presence of the electrolytes/salts. The conformational change of the polymer affects the properties of the hydrogels. To have a better understanding of the mechanical properties of the hydrogel, viscoelastic and swelling properties of PHisMA hydrogel were studied at different pH conditions. PHisMA hydrogels were prepared by UV-induced free radical polymerization. After equilibration in the sodium acetate buffer at different pHs, the hydrogels were characterized using the rheological technique. Hydrogels were studied by two rheological measurements: (1) the strain-sweep measurement under a certain frequency obtained from the frequency-sweep experiment suggests that subsequent time sweeps are carried out in the linear viscoelastic region, and does not influence the gel network structure; (2) a frequency-sweep measurement using small strain allows us to determine the equilibrium modulus under different pH environments.

Figure 4 shows storage modulus and loss modulus of PHisMA hydrogels at various pH conditions (pH 3, pH 4, pH 5 and pH 7). The equilibrium moduli (Table 2) indicate that the viscoelastic properties of PHisMA hydrogel in the zwitterionic state are much higher than those in the cationic and anionic states. In the low ionic strength solution, zwitterionic polymer

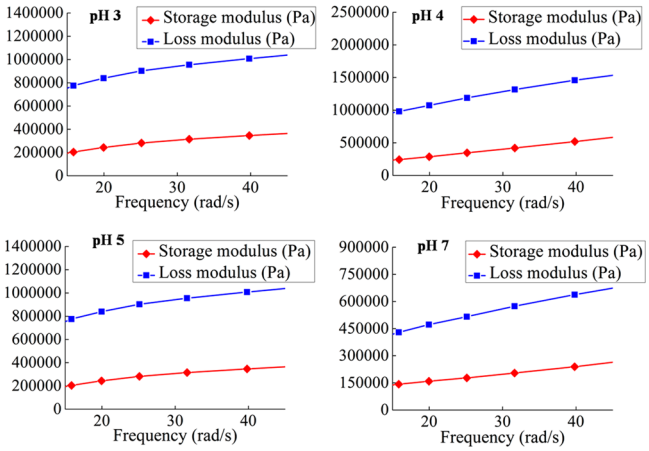

Figure 4. Rheological studies of PHisMA hydrogels. Frequency sweep conducted under 10% strain and 100−0.1 rad/s using 25 mm parallel plate.

Table 2. Equilibrium Modulus and Swelling Ratio of PHisMA Hydrogels under Different pH Conditions (pH 3, pH 4, pH 5, and pH 7)

	equilibrium modulus (Pa)	swelling ratio (%)
pH 3	8 000	1259.73
pH 4	150 000	324.12
pH 5	60 000	768.37
pH 7	35 000	1108.96

collapses and aggregates due to interchain and intrachain electrostatic attractions, which lead to higher cross-linking density of the hydrogel. For the hydrogel at anionic or cationic states, PHisMA polymer chains are stretched due to the repulsive force among charged groups, which results in lower cross-linking density and viscoelastic properties. The equilibrium modulus of PHisMA hydrogel at the cationic state is lower than that at the anionic state. This phenomenon can be caused by the different cross-linking density caused by a higher degree of hydrogen bond contributed by uncharged imidazole groups or the osmotic activities of the different counterions around the charged groups. The results from rheological studies point out that zwitterionic polymers have higher equilibrium modulus and higher cross-linking density owing to stronger inter- and intrachain interaction, whereas the anionic and cationic PHisMA show lower viscoelastic properties due to the inter- and intrachain repulsion.

The swelling ratios of PHisMA hydrogels in buffers at different pH values (pH 3, pH 4, pH 5, and pH 7) were consistent with rheological data. As shown in Table 2, the water uptakes of anionic and cationic PHisMA hydrogels are much higher than that at the zwitterionic state. The charges within zwitterionic hydrogels can act as reversible cross-linkers resulting in variations of the effective network density. The electrostatic interactions between either opposite charges or dipole−dipole pairs in zwitterionic hydrogels lead to higher cross-linking density in the polymer network. Our study demonstrated that we could control the swelling properties of the hydrogel by adjusting the pH of the solution. The pH sensitive hydrogels can potentially be used as pH actuators for sensors and devices.

The capability of polyelectrolytes to chelate metal ions is particularly attractive for biofilm management, wound healing and environmental applications. Since both carboxylate and imidazole are common chelating groups, we expect that PHisMA is able to chelate high-valent metal ions. The chelating capability of PHisMA hydrogel on multi-valent metal ions (Ca^{2+}, Mg^{2+},Cu^{2+}, Ni^{2+} and Fe^{3+}) were investigated in this study. The amounts of metal ions absorbed by PHisMA were calculated and are shown in Table 3. The images of PHisMA hydrogels after chelation with Cu^{2+}, Ni^{2+} and Fe^{3+} are displayed in Figure 5. Among all tested metal ions, PHisMA has strong binding affinity to +2 and +3 metal ions. Notably, the control of free metal ions is extremely important for biofilm/infection management. Of medical importance, biofilm can withstand attack from the immune system and resist antibiotic/biocide treatments. The treatment of biofilm is one of the most important medical and environmental challenges. A previous study unveiled that magnesium, calcium and iron ions play a significant role in the development of *Pseudomonas aeruginosa* biofilm, which is one of the major species causing hospital

Table 3. Binding Capacity of PHisMA Hydrogel to Calcium Chloride, Magnesium Sulfate, Copper(II) Chloride, Nickel(II) Sulfate, and Ferric Chloride

cation	D (mmol/g)
calcium(II)	1.82
magnesium(II)	3.03
copper(II)	2.86
nickel(II)	3.02
iron(III)	2.87

DOI: 10.1021/acs.langmuir.6b01465
Langmuir XXXX, XXX, XXX−XXX

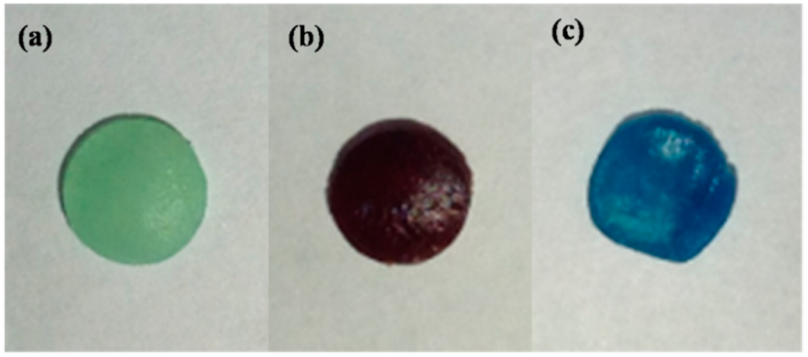

Figure 5. Images of PHisMA hydrogels after chelation with (a) nickel(II), (b) iron(III), and (c) copper(II) ions.

infections, and the removal of the high-valent ions can prevent biofilm formation and decrease the viability of the biofilm.[47] Since PHisMA can chelate multi-valent metal ions, PHisMA may potentially inhibit biofilm formation by reducing the amount of the free metal ions in the wound. Further biofilm formation experiments will be examined in the future.

4. CONCLUSION

We synthesized the amino acid based pH-responsive PHisMA material, which is capable of switching among zwitterionic, anionic and cationic forms, reducing adsorption of proteins and inhibiting cell adhesion at its zwitterionic state, carrying tunable viscoelastic properties, water uptakes and chelation capability to multi-valent metal ions. Through this study, we established a better understanding of structure−property relationships of zwitterionic PHisMA. We were able to obtain the desired properties by adjusting the pH of the system. This material may be an excellent candidate for wound treatment, gene delivery, and membrane and protein purifications, which require controllable fouling/antifouling properties at complex interfaces and chelation effect with high-valent metal cations.

AUTHOR INFORMATION

Corresponding Author

*E-mail: gc@uakron.edu. Fax: 330-972-7250. Web: http://gozips.uakron.edu/~gc/index.html.

Notes

The authors declare no competing financial interest.

ACKNOWLEDGMENTS

This work is supported by the U.S National Science Foundation (ECCS-1200032, DMR-1206923 and DMR-1454837) and the Natural Science Foundation of China (NSFC-51528301).

REFERENCES

(1) Rosenhahn, A.; Schilp, S.; Kreuzer, H. J.; Grunze, M. The Role of "Inert" Surface Chemistry in Marine Biofouling Prevention. *Phys. Chem. Chem. Phys.* **2010**, *12*, 4275−4286.

(2) Ratner, B. D.; Bryant, S. J. Biomaterials: Where We Have Been and WhereWe Are Going. *Annu. Rev. Biomed. Eng.* **2004**, *6*, 41−75.

(3) Suh, J. K. F.; Matthew, H. W. T. Application of Chitosan-based Polysaccharide Biomaterialsin Cartilage Tissue Engineering: a Review. *Biomaterials* **2000**, *21*, 2589−2598.

(4) Madihally, S. V.; Matthew, H. W. T. Porous Chitosan Scaffolds for Tissue Engineering. *Biomaterials* **1999**, *20*, 1133−1142.

(5) Langer, R. Drugs on Target. *Science* **2001**, *293*, 58−59.

(6) Peer, D.; Karp, J. M.; Hong, S.; Farokhzad, O. C.; Margalit, R.; Langer, R. Nanocarriers as an Emerging Platform for Cancer Therapy. *Nat. Nanotechnol.* **2007**, *2*, 751−760.

(7) Janes, K. A.; Calvo, P.; Alonso, M. J. Polysaccharide Colloidal Particles as Delivery Systems for Macromolecules. *Adv. Drug Delivery Rev.* **2001**, *47*, 83−97.

(8) Agnihotri, S. A.; Mallikarjuna, N. N.; Aminabhavi, T. M. Recent Advances on Chitosan-based Micro- and Nanoparticlesin Drug Delivery. *J. Controlled Release* **2004**, *100*, 5−28.

(9) Qiu, Y.; Park, K. Environment-sensitive Hydrogels for Drug Delivery. *Adv. Drug Delivery Rev.* **2001**, *53*, 321−339.

(10) Calvo, A.; Yameen, B.; Williams, F. J.; Soler-Illia, G. J. A. A.; Azzaroni, O. Mesoporous Films and Polymer Brushes Helping Each Other To ModulateIonic Transport in Nanoconfined Environments. An Interesting Example of Synergism in Functional Hybrid Assemblies. *J. Am. Chem. Soc.* **2009**, *131*, 10866−10868.

(11) Van Reis, R.; Zydney, A. Membrane separations in biotechnology. *Curr. Opin. Biotechnol.* **2001**, *12*, 208−211.

(12) Van Reis, R.; Zydney, A. Bioprocess membrane technology. *J. Membr. Sci.* **2007**, *297*, 16−50.

(13) Vaisocherova, H.; Zhang, Z.; Yang, W.; Cao, Z.; Cheng, G.; Taylor, A. D.; Piliarik, M.; Homola, J.; Jiang, S. FunctionalizableSurface Platform with Reduced Nonspecific Protein Adsorption from Full Blood Plasma—Material Selection and Protein Immobilization Optimization. *Biosens. Bioelectron.* **2009**, *24*, 1924−1930.

(14) Jelinek, R.; Kolusheva, S. Carbohydrate Biosensors. *Chem. Rev.* **2004**, *104*, 5987−6015.

(15) Collings, A. F.; Caruso, F. Biosensors: Recent Advances. *Rep. Prog. Phys.* **1997**, *60*, 1397−1445.

(16) Jhong, J. F.; Venault, A.; Liu, L.; Zheng, J.; Chen, S. H.; Higuchi, A.; Huang, J.; Chang, Y. Introducing Mixed-Charge Copolymers As Wound Dressing Biomaterials. *ACS Appl. Mater. Interfaces* **2014**, *6*, 9858−9870.

(17) Cao, B.; Li, L.; Wu, H.; Tang, Q.; Sun, B.; Dong, H.; Zhe, H.; Cheng, G. Zwitteration of Dextran: a Facile Route to Integrate Antifouling, Switchability and Optical Transparencyinto Natural Polymers. *Chem. Commun.* **2014**, *50*, 3234−3237.

(18) Jiang, S.; Cao, Z. Ultralow-Fouling, Functionalizable, and HydrolyzableZwitterionic Materials andTheir Derivatives forBiological Applications. *Adv. Mater.* **2010**, *22*, 920−932.

(19) Cheng, G.; Mi, L.; Cao, Z.; Xue, H.; Yu, Q.; Carr, L.; Jiang, S. Functionalizable and Ultrastable Zwitterionic Nanogels. *Langmuir* **2010**, *26*, 6883−6886.

(20) Cheng, G.; Li, G.; Xue, H.; Chen, S.; Bryers, J. D.; Jiang, S. Zwitterionic Carboxybetaine Polymer Surfaces and Their Resistance to Long-term Biofilm Formation. *Biomaterials* **2009**, *30*, 5234−5240.

(21) Keefe, A. J.; Jiang, S. Poly(zwitterionic) Protein Conjugates Offer Increased Stability Without Sacrificing Binding Affinity or Bioactivity. *Nat. Chem.* **2012**, *4*, 59−63.

(22) Sundaram, H. S.; Ella-Menye, J. R.; Brault, N. D.; Shao, Q.; Jiang, S. Reversibly Switchable Polymer with Cationic/Zwitterionic/Anionic Behavior Through Synergistic Protonation and Deprotonation. *Chem. Sci.* **2014**, *5*, 200−205.

DOI: 10.1021/acs.langmuir.6b01465
Langmuir XXXX, XXX, XXX−XXX

(23) Ostuni, E.; Chapman, R. G.; Holmlin, R. E.; Takayama, S.; Whitesides, G. M. A Survey of Structure-Property Relationships of Surfacesthat Resist the Adsorption of Protein. *Langmuir* **2001**, *17*, 5605−5620.
(24) Herold, D. A.; Keil, K.; Bruns, D. E. Oxidation of Polyethylene Glycols by Alcohol Dehydrogenas. *Biochem. Pharmacol.* **1989**, *38*, 73−76.
(25) Harder, P.; Grunze, M.; Dahint, R.; Whitesides, G. M.; Laibinis, P. E. Molecular Conformation in Oligo(ethylene glycol)-Terminated Self-Assembled Monolayerson Gold and Silver Surfaces Determines Their Ability To Resist Protein Adsorption. *J. Phys. Chem. B* **1998**, *102*, 426−436.
(26) Shen, M. C.; Martinson, L.; Wagner, M. S.; Castner, D. G.; Ratner, B. D.; Horbett, T. A. PEO-like Plasma Polymerized TetraglymeSurface Interactions with Leukocytes and Proteins:*in vitro* and *in vivo* Studies. *J. Biomater. Sci., Polym. Ed.* **2002**, *13*, 367−390.
(27) Li, L.; Chen, S.; Jiang, S. Protein Interactions with OligoethyleneGlycol OEG Self-assembled Monolayers OEG Stability, Surface Packing Density and Protein Adsorption. *J. Biomater. Sci., Polym. Ed.* **2007**, *18*, 1415−1427.
(28) Gaberc-Porekar, V.; Zore, I.; Podobnik, B.; Menart, V. Obstacles and Pitfalls in the PEGylation of Therapeutic Proteins. *Curr. Opin. Drug. Discovery Dev.* **2008**, *11*, 242−250.
(29) Chen, S.; Zheng, J.; Li, L.; Jiang, S. Strong Resistance of Phosphorylcholine Self-Assembled Monolayers to Protein Adsorption: Insights into Nonfouling Properties of Zwitterionic Materials. *J. Am. Chem. Soc.* **2005**, *127*, 14473−14478.
(30) Leckband, D.; Sheth, S.; Halperin, A. Grafted Poly(ethylene oxide) Brushes as Nonfouling Surface Coatings. *J. Biomater. Sci., Polym. Ed.* **1999**, *10*, 1125−1147.
(31) He, Y.; Hower, J.; Chen, S.; Bernards, M. T.; Chang, Y.; Jiang, S. Molecular Simulation Studies of Protein Interactions with Zwitter-ionicPhosphorylcholine Self-Assembled Monolayers in the Presence ofWater. *Langmuir* **2008**, *24*, 10358−10364.
(32) Liu, Q.; Singh, A.; Liu, L. Amino Acid-Based Zwitterionic Poly(serine methacrylate) as an Antifouling Material. *Biomacromolecules* **2013**, *14*, 226−231.
(33) Bauri, K.; Roy, S. G.; Pant, S.; De, P. Controlled Synthesis of Amino Acid-Based pH-Responsive Chiral Polymers and Self-Assembly of Their Block Copolymers. *Langmuir* **2013**, *29*, 2764−2774.
(34) Sanda, F.; Endo, T. Syntheses and Functions of Polymers Based on Amino Acids. *Macromol. Chem. Phys.* **1999**, *200*, 2651−2661.
(35) Klok, H. A.; Langenwalter, J. F.; Lecommandoux, S. Self-Assembly of Peptide-Based Diblock Oligomers. *Macromolecules* **2000**, *33*, 7819−7826.
(36) Nicolas, J.; Mantovani, G.; Haddleton, D. M. Living Radical Polymerization as a Tool for the Synthesis of Polymer-Protein/PeptideBioconjugates. *Macromol. Rapid Commun.* **2007**, *28*, 1083−1111.
(37) Geng, Y.; Discher, D. E.; Justynska, J.; Schlaad, H. Grafting Short Peptides onto Polybutadiene-block-poly(ethylene oxide): A Platform forSelf-Assembling Hybrid Amphiphiles. *Angew. Chem., Int. Ed.* **2006**, *45*, 7578−7581.
(38) O'Reilly, R. K. Using Controlled Radical Polymerization Techniques for the Synthesis of FunctionalPolymers Containing Amino Acid Moieties. *Polym. Int.* **2010**, *59*, 568−573.
(39) Lee, J.; Wu, H.; Tang, Q.; Cao, B.; Wang, H.; Cong, H.; Zhe, J.; Xu, F.; Cheng, G. Structure−Function Relationships of a Tertiary Amine-Based Polycarboxybetaine. *Langmuir* **2015**, *31*, 9965−9972.
(40) Ishii, T.; Wada, A.; Tsuzuki, S.; Casolaro, M.; Ito, Y. Copolymers Including L-Histidine and Hydrophobic Moiety for-Preparation of Nonbiofouling Surface. *Biomacromolecules* **2007**, *8*, 3340−3344.
(41) Benetti, E. M.; Zapotoczny, S.; Vancso, G. J. Tunable Thermoresponsive Polymeric Platforms on Gold by "Photoiniferter"-Based Surface Grafting. *Adv. Mater.* **2007**, *19*, 268−271.
(42) Cheng, G.; Xue, H.; Zhang, Z.; Chen, S.; Jiang, S. A Switchable Biocompatible Polymer Surface with Self-Sterilizing and Nonfouling Capabilities. *Angew. Chem., Int. Ed.* **2008**, *47*, 8831−8834.
(43) Tiller, J. C.; Liao, C.; Lewis, K.; Klibanov, A. M. Designing Surfaces that Kill Bacteria on Contact. *Proc. Natl. Acad. Sci. U. S. A.* **2001**, *98*, 5981−5985.
(44) Vigeant, M. A. S.; Ford, R. M.; Wagner, M.; Tamm, L. K. Reversible and Irreversible Adhesion of Motile *Escherichia coli* Cells Analyzed by Total Internal Reflection Aqueous Fluorescence Microscopy. *Appl. Environ.Microb.* **2002**, *68*, 2794−2801.
(45) Shrager, R. I.; Cohen, J. S.; Heller, S. R.; Sachs, D. H.; Schechter, A. N. Nuclear Magnetic Resonance Titration Curves of Histidine Ring Protons. *Biochemistry* **1972**, *11*, 541−547.
(46) Hermansson, M. The DLVO Theory in Microbial Adhesion. *Colloids Surf., B* **1999**, *14*, 105−119.
(47) Banin, E.; Brady, K. M.; Greenberg, E. P. Chelator-Induced Dispersal and Killing of *Pseudomonas aeruginosa* Cells in a Biofilm. *Appl. Environ. Microb.* **2006**, *72*, 2064−2069.

DOI: 10.1021/acs.langmuir.6b01465
Langmuir XXXX, XXX, XXX−XXX